Centrifuge modelling of piled structure response to tunnelling

A. Franza & A.M. Marshall
University of Nottingham, Nottingham, UK

ABSTRACT: In urban areas, tunnelling may compromise existing piled structures. In this paper, centrifuge tests performed to investigate the effects of tunnelling in sands on piled buildings are described. Piled buildings were modelled in the centrifuge as an aluminium plate with varying stiffness supported by aluminium piles. Ground movements and plate displacements were measured using an image-based measurement technique. Tunnelling-induced vertical and horizontal displacement profiles of the superstructure were compared with greenfield surface and subsurface ground movements. The variation of the building settlement profiles with plate stiffness and tunnel volume loss illustrates the main effects of tunnel-pile interaction (TPI) and the contribution of the superstructure stiffness to the global tunnel-pile-structure interaction (TPSI). Furthermore, results confirm that the axial stiffness of piled buildings prevents significant horizontal strains of the superstructure. Finally, the potential for damage is studied by comparing the building and greenfield deflection ratios. It is illustrated that piled foundations alter the global tunnel-building interaction where the piles have a detrimental role in TPSI problems, whereas the stiffness of buildings can significantly reduce the resulting building distortions.

1 INTRODUCTION

Current needs for infrastructure and services in urban areas often require the construction of tunnels that may affect existing structures. In the case of piled buildings, to preserve structural serviceability and safety, it is necessary to assess the structural distortions caused by tunnelling. Despite its practical importance, tunnelling beneath piled building, which induces pile settlements that are a primary source of damage, has not been adequately investigated.

Previous works on tunnel-structure interaction (TSI) in the case of shallow foundations recognised the importance of the building stiffness which tends to decrease the structural distortions (Fargnoli et al. 2015, Farrell et al. 2014, Franzius et al. 2006, Giardina et al. 2015). The building deflection ratio, *DR*, and the horizontal strains, ε^h, were used as indicators of the building deformations because they allow for a preliminary building damage assessment based on the limiting tensile strain method. To derive the resulting building *DR* values from the greenfield settlement trough, the deflection ratio modification factors, M^{DR}, are used, which are defined and illustrated in Figure 1. Note that the location of the inflection points, i and i_{bldg}, may vary with tunnel volume loss, $V_{l,t}$, whereas *DR* is calculated based on the maximum relative deflection, Δ.

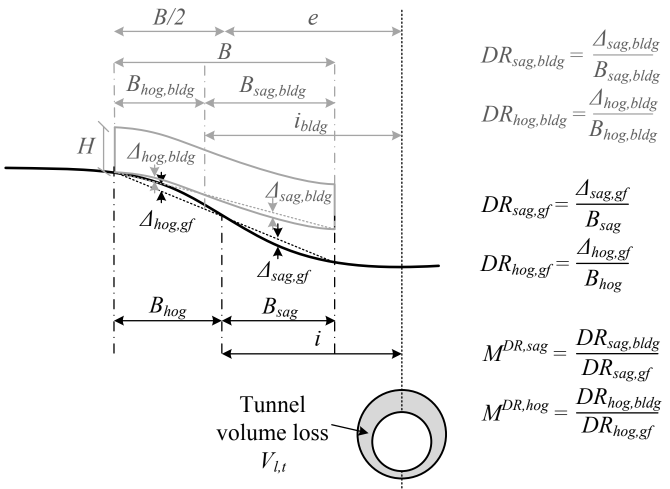

Figure 1. Relative deflection, Δ, and deflection ratio, *DR*, based on a generic greenfield settlement profile and structural settlement curves.

The interaction problem between the tunnel and a single pile or pile group have been analysed using field trials as well as physical and numerical modelling, leading to some confidence in the assessment of pile group displacements and pile failure due to tunnelling (Basile 2014, Jacobsz et al. 2004, Kaalberg et al. 2005, Marshall & Mair 2011).

Few studies have been conducted to understand the global tunnel-pile-structure interaction (TPSI) and limited indications are available to conduct damage risk assessments of piled structures. In practice, engineers may evaluate the tunnelling-induced deformations of piled buildings with empirical TPI analyses assuming that pile heads settle as the subsurface greenfield settlement trough at the depth, z, equal to 2/3 of the pile length, L_p (Devriendt & Williamson 2011). However, assessing tunnelling-induced deformations in buildings from TPI (i.e. assuming a fully flexible building) neglects the building influence on the global interaction and may be overly conservative, as illustrated by the case study reported by Goh & Mair (2014).

In this paper, a series of centrifuge tests performed to investigate the response of piled buildings to tunnelling in sands is described.

2 EXPERIMENTAL SET UP, TEST PREPARATION AND REPEATABILITY

The tests were performed at 80 g using the University of Nottingham geotechnical centrifuge. In the following, both the model dimensions and results are reported in model scale. The model layout is shown in Figure 2.

The experimental package developed by Zhou et al. (2014) to model the greenfield tunnelling process in plane strain conditions was used. A 90 mm diameter model tunnel buried at 225 mm depth (at axis) was adopted to replicate a prototype 7.2 m diameter tunnel with 14.4 m of cover (C/D = 2). The inside plan dimensions of the strong box are 640 × 260 mm and the maximum height of soil within the box is 500 mm. A dry silica sand known as Leighton Buzzard Fraction E with d_{50} = 0.122 mm was used for testing. The tunnel comprised a rubber membrane filled with water. It consisted of an eccentric cylinder with enlarged ends covered by a latex sleeve sealed with O-rings. A tunnel volume control system comprising a constant-head standpipe, a solenoid valve, a linear actuator, a water-filled sealed cylinder and an LVDT was used. The tunnel volume loss process was conducted in 0.25 % increments up to 5 % and, subsequently, 0.5 % increments up to 10 %. Note that this set up does not allow modelling tunnel excavation progress in the longitudinal direction.

A piled building was modelled in the centrifuge using aluminium plates with varying stiffness supported by aluminium piles (E = 70 GPa). The piled foundation consisted of two transverse pile rows of seven piles. During each test, the plate, with a transverse width B = 500 mm and a length L = 256 mm, was placed centrally with respect to the tunnel centreline. Four different plate thicknesses, t, were used: 1.6, 3, 6 and 12.3mm. As a result of the varying plate thickness, the weight of the building also varied between tests. This impacts on results, which will be discussed later and will be the focus of future testing.

Several tests were repeated to evaluate the repeatability of results. Tests are labelled according to the plate thickness and repeated test indicator (i.e. second test performed with a 6 mm thick plate is referred to as t6.b). A fully elastic response is expected for this type of building model whose axial and flexural stiffness at prototype scale is comparable with real case scenarios (Farrell 2014). Prototype axial and flexural stiffnesses are summarised in Table 1.

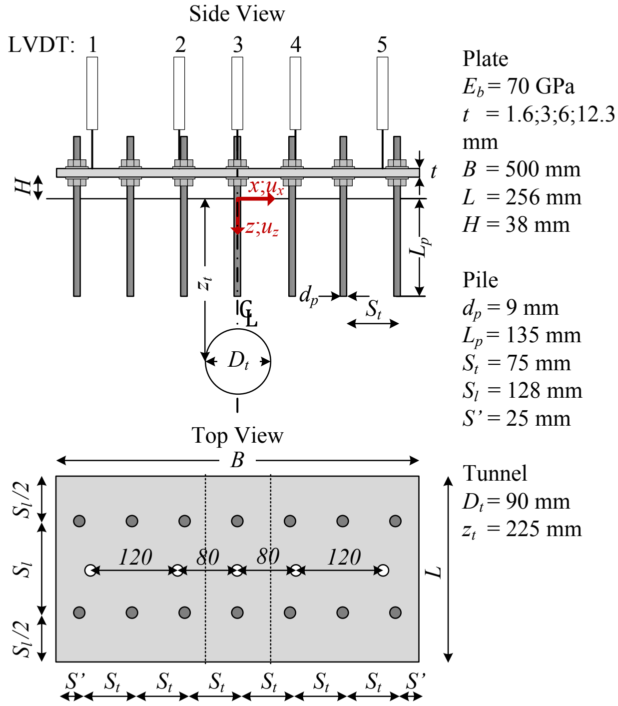

Figure 2. Test layout (in scale).

Table 1. Stiffness of the aluminium plates.

Test	Model Scale		Prototype scale			
	t (mm)	S_l (mm)	t (m)	S_l (m)	EI^* (kNm^2/m)	EA^* (kNm^2/m)
GF			Greenfield			
t1. a	1.6	128	0.13	10.2	1.2×10^4	9.0×10^6
t3. a-b-c	3	128	0.24	10.2	8.1×10^4	1.7×10^7
t6. a-b-c	6	128	0.48	10.2	6.5×10^5	3.4×10^7
t12.a	12.3	128	0.98	10.2	5.6×10^6	6.9×10^7

Note that the model did not satisfy plain strain condition. However, the longitudinal length L of the model building (256 mm) was approximately equal to the strongbox width (260 mm) and the pile row spacing in the longitudinal direction, S_l, equal to 128mm (10.24 m at prototype scale), was double the pile row distance from the building edges; therefore the Perspex wall and the back wall of the strongbox approximately represent planes of symmetry. This means that the centrifuge tests modelled the behaviour of an infinitely long building in the longitudinal direction (limited in the model to a portion corresponding to two pile rows) subjected to the ground movements due to plain strain tunnel volume loss distribution (replicating the steady state condition obtained behind the tunnel face).

The model piles consisted of 8 mm diameter aluminium alloy full section round bar over a length of 220 mm. Piles had a fully rough interface obtained by bonding fraction E sand to the outer surface. The final external pile diameter was 9 mm and the embedment depth was 135 mm (corresponding, respectively, to 0.72 m and 10.8 m at prototype scale). The additional pile length allowed for a gap between the plate and the soil, H, of 38 mm as well as for a threaded pile top, which was used to rigidly attach the piles to the plate (simulating fixed pile-foundation connections).

Two digital cameras were used to take pictures of the soil (during test GF) and the plate at the front Perspex wall of the centrifuge container. During the test, digital photos were taken at each $V_{l,t}$ increment. To measure soil and plate displacements, the geoPIV image-based measurement technique was used (White et al. 2003). Plate settlements were also monitored with a row of five LVDTs located at a horizontal distance from the tunnel centreline of 0, ±80 and ±200 mm (Fig. 2).

A simplified test preparation procedure that achieved good repeatability of results was adopted in order to reduce the preparation time. [1] With the experimental package mounted on the centrifuge, the sand was manually poured to a relative density, I_d, of 30±5 %, starting from the tunnel springline level. The effects of sand pouring only above the tunnel springline was considered negligible because previous greenfield centrifuge tests displayed that tunnel deformations are localised at the top half of the model tunnel. [2] The plate was installed prior the spin up by jacking the plate-piled foundation to the designed depth, which allowed for a gap between soil and building. Therefore, the model replicated a piled foundation rather than a piled-raft foundation. Considering the aim of obtaining an overall loose soil sample without an entirely accurate control of I_d, the effects of driving the piled foundation at 1g on I_d were neglected. [3] The model was spun-up to the level of 80g. [4] Once the target g-level was reached, the tunnelling process was modelled in-flight and plate deformations were measured with the PIV technique. [5] At the conclusion of the $V_{l,t}$ process, the centrifuge was spun down; the piled plate and the sand up to the tunnel depth z_t were removed and the model tunnel was filled back with the water extracted during phase [4].

To illustrate that good repeatability of results was achieved, two different piled building configurations were tested three times (configuration t3 and t6). The building displacements measured with the PIV technique and the LVDTs during the centrifuge tests are compared in Figure 3. Results display good repeatability within a test series (compare Figs. 3c, d, e and Figs. 3f, g, h) and good agreement between PIV measured settlements and LVDT readings. However, note that the higher the plate stiffness, the greater the difference between PIV and LVDT measurements (PIV data being greater). This can be partly explained by non-uniform deformations across the length L of the plate, which does not act as a perfect beam under the actions of the attached piles. This hypothesis was confirmed by elastic finite element analyses of the plate.

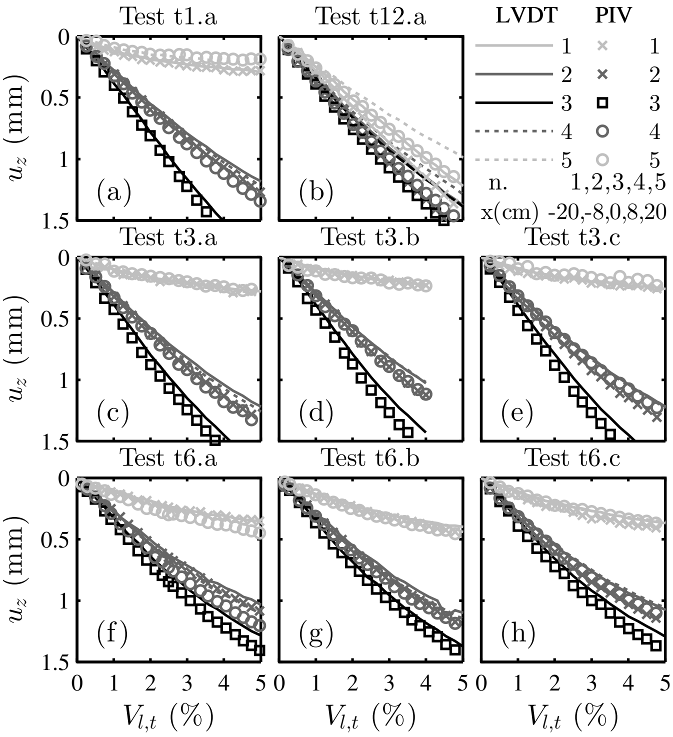

Figure 3. PIV and LDVT measurements of plate settlements.

Furthermore, results shown in Figure 3 illustrate a gradual reduction of the plate settlement increment rate with $V_{l,t}$, which is more marked for the configuration t6 than for tests t3 and t1. This reduction of plate settlement increment rate with $V_{l,t}$ is probably due to soil plasticity and ground stiffness degradation due to tunnelling and TPSI mechanisms (i.e. the building displaces the piles because of its own stiffness, inducing additional shearing strains at the soil-pile interface). On the contrary, the plate settlement increment rate measured during test t12 is approximately constant (Fig. 3b) and higher than the rates measured during by tests t1, 3 and 6. Further remarks regarding test t12 are provided in the following section to provide an explanation for this phenomenon.

3 CENTRIFUGE MODELLING RESULTS

A comparison of the vertical (u_z) and horizontal (u_x) displacement curves of the plates measured at $V_{l,t}$ = 1 and 5 % is presented in Figure 4. For comparison, greenfield displacement curves at z = 0 and z/L_p = 2/3 are also shown. Building displacement curves

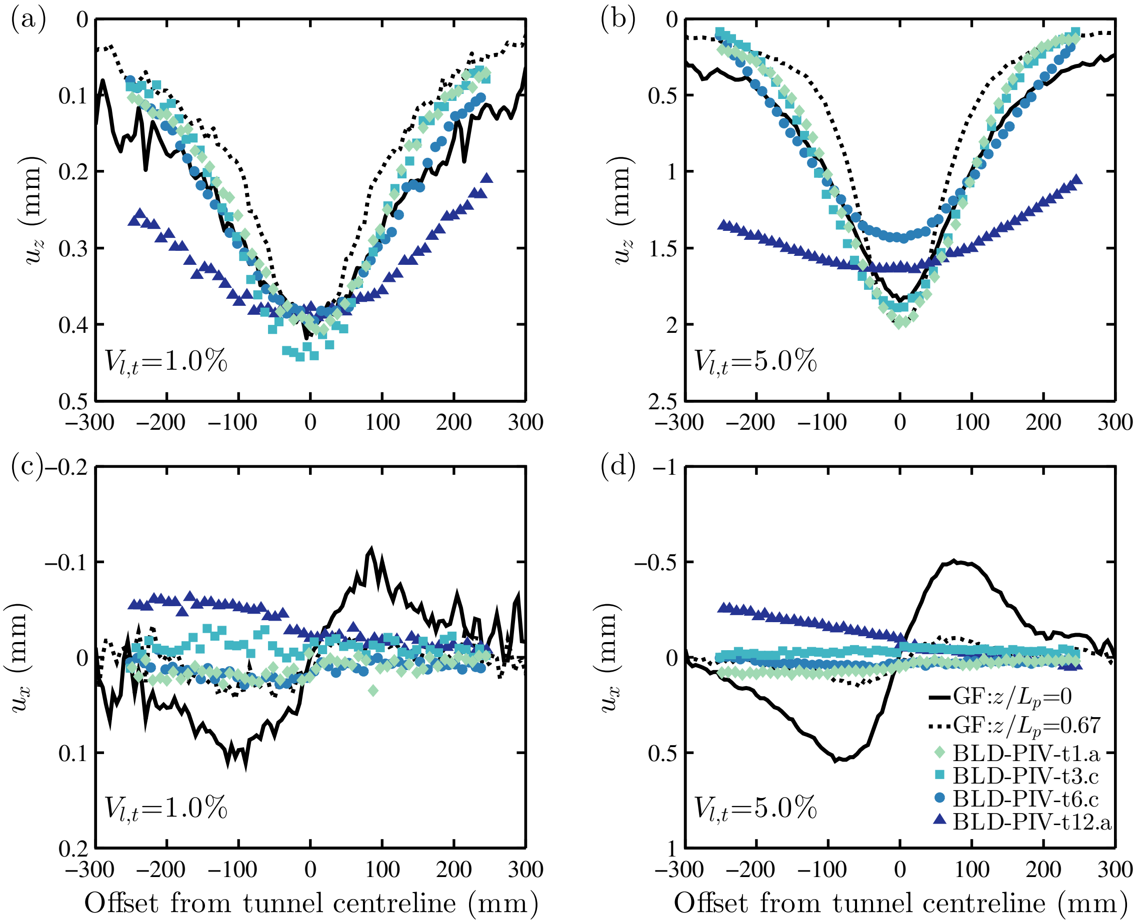

Figure 4. Vertical and horizontal displacements of the piled plates measured by PIV.

were approximately symmetric except for test t12, which showed by higher displacements on the left side and a global horizontal translation of the plate towards right (i.e. linear trend of horizontal movements with x).

The variation of the building settlement curves with plate stiffness t and $V_{l,t}$ in Figures 4a, b illustrates the main effects of tunnel-pile interaction (TPI) and the contribution of the superstructure stiffness to the global tunnel-pile-structure interaction (TPSI). To understand the TPI, it is necessary to analyse the response of flexible superstructures, where the superstructure influence is minimum. The settlement curves of t1 and t3 are characterised by having both hogging and sagging regions and a settlement curve that is intermediate between the surface and subsurface greenfield settlement troughs. These centrifuge outcomes confirm that the TPI mechanism is due to the interaction of the piles with subsurface ground movements along the pile axis and that isolated piles with their tips above the tunnel should settle more than the surface, whereas piles outside this region should settle less than the surface. This leads to an increase of the relative deflection of the fully-flexible structures compared to shallow foundations that would deform according to surface greenfield settlement troughs.

On the other hand, the effects of the plate stiffness increment, which is evident for the stiffest building, t12, are (i) the reduction of the plate relative deflection, Δ, and (ii) a decrease of the portion of the plate undergoing the secondary deformation mode (i.e. hogging deformations for building centred above the tunnel) due to the increase of i_{bldg} (defined in Fig. 1). Effect (i) is due to the plate resisting the central deflection through its own stiffness and the residual bearing capacity of the external piles (i.e. those furthest from the tunnel), which is a function of the weight of the plate. To restrain the downwards movement of the central piles, the plate applies tensile axial forces (due to tunnelling) near the pile head of the central piles, resulting in an upwards pile movement relative to the soil. The plate redistributes load to the external piles, which are consequently driven into the soil. In the case of buildings with a self-weight, this mechanism would induce a redistribution of the loads towards the external piles. If the total load after tunnelling on an external pile increases to the residual pile bearing capacity, the pile (and entire plate) undergoes significant settlements, as illustrated in Fig. 4c for test t12. Future tests are planned in which the building stiffness is varied whilst maintaining constant building weight order to better isolate the effect of building stiffness. Effect (ii) was also noticed by Farrell et al. (2014), who performed centrifuge tests to study the deformations induced by tunnelling on a plate. Overall, effects (i) and (ii) result in a reduction of the building distortions with plate thickness t.

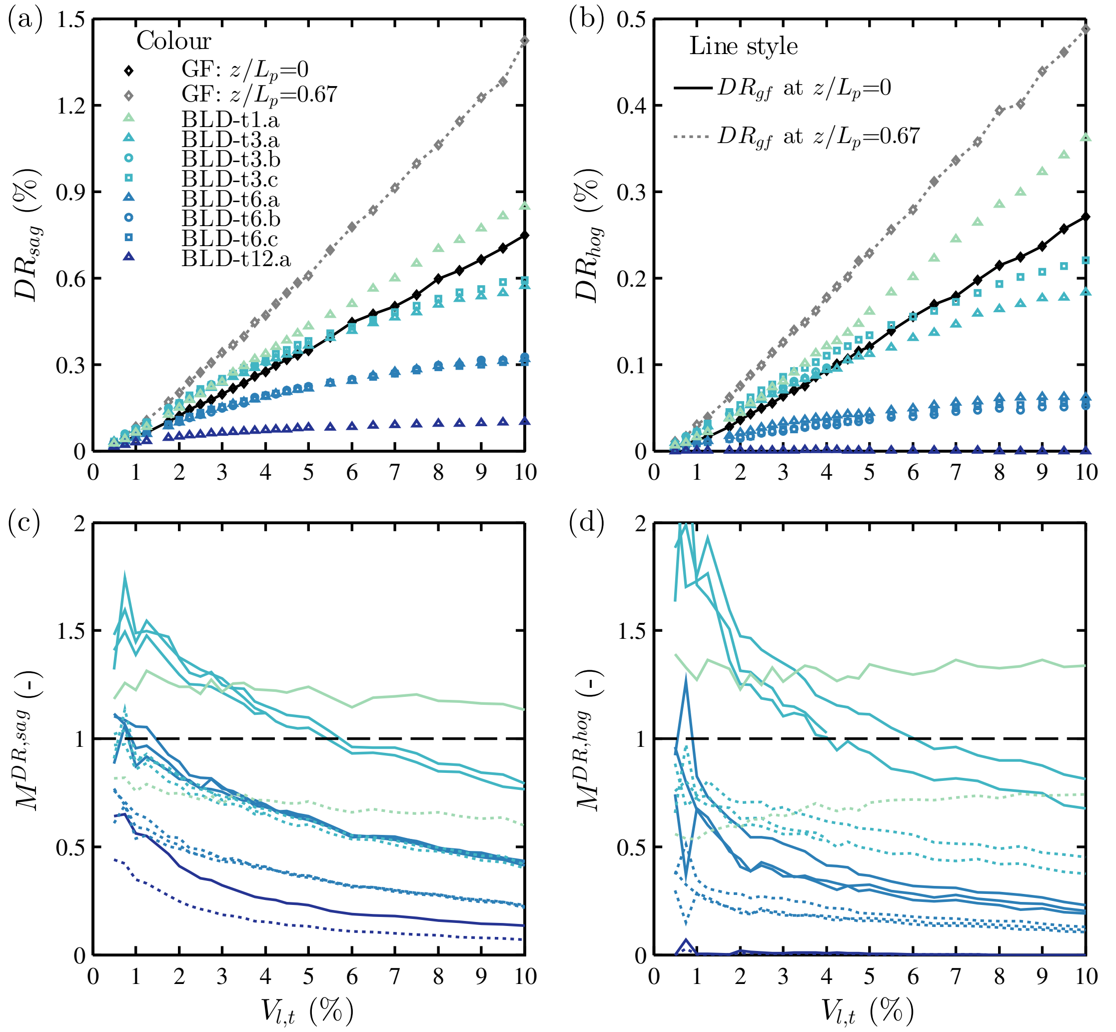

Figure 5. Deflection ratios and modification factors in sagging and hogging

Figures 4c, d show the horizontal displacements of the plates. Despite the scatter of the data, the results displayed in these figures confirm that the axial stiffness of the superstructure prevents significant horizontal strains of the superstructure (i.e. horizontal displacement curves show approximately a linear trend with the horizontal offset *x*). These outcomes agree with the findings of previous researches indicating negligible horizontal strains for buildings on continuous footings. However, these conclusions should not be generalised to buildings without horizontal structural elements connecting the pile heads (Goh & Mair 2014).

The influence of the superstructure and $V_{l,t}$ on deflection ratios, *DR*, and modification factors, M^{DR}, is displayed in Figure 5. To calculate *DR* and the location of the inflection points, *i* and i_{bldg}, the settlement data were interpolated with modified Gaussian curves (Farrell et al. 2014). Figures 5a, b display the building and greenfield *DR*s in both sagging and hogging. Firstly, it is important to note the clear linear trend of *DR* with $V_{l,t}$ for tests GF and t1. Previous researchers have illustrated that greenfield settlement troughs in sands become narrower with the increase of $V_{l,t}$ and suggested that a narrow settlement trough with large maximum settlement poses higher potential for damage to structures (Franza and Marshall 2015, Marshall et al. 2012). However, for test GF, $DR_{gf,sag}$ and $DR_{gf,hog}$ have approximately linear trends with $V_{l,t}$, rather than increasing nonlinearly (exponentially) due to the narrowing of the settlement curves. Note that the DR_{gf} - $V_{l,t}$ relationship should be linear when the shape of the settlement curve does not change with $V_{l,t}$ (typical for undrained clay where volumetric strains are zero). Therefore, the linear trend of DR_{gf} - $V_{l,t}$ during test GF is likely due to the combination of the decrease of *i* combined with the effects of the volumetric strains. Further investigations are needed to fully understand the effects of I_d, *C/D, B* and *e/B* on the DR_{gf} - $V_{l,t}$ relationship in sands. Secondly, the *DR*s measured during test t1 are intermediate between greenfield surface and subsurface values. This confirms the averaging effect of piles on greenfield soil movements. Figures 5a, b also show results for the centrifuge tests t3, 6 and 12. These data follow nonlinear distributions that are characterised by decreasing values of *DR* with plate thickness *t* and a gradual decrease of the increment rate with $V_{l,t}$, which results in an asymptotic trend of *DR* at high volume loss. Interestingly, the higher the value of *t*, the lower the value of $V_{l,t}$ at which a steady trend of *DR* is reached. As discussed previously for the results in Figure 3, the observed non-linear trend of the superstructure distortions with volume loss could be attributed to the progressive degradation of the soil stiffness and the relative pile-soil displacements induced by the superstructure.

Figures 5c, d show the reduction factors, $M^{DR,sag}$ and $M^{DR,hog}$, calculated using surface (solid lines) and subsurface (dashed lines) greenfield settlements. From these data, it is apparent that the TPI mechanism results in M^{DR} values greater than unity for flexible structures, whereas structural stiffness contributes to a decrease of the flexural deformations (as discussed earlier). The plots show approximately constant modification factors M^{DR} for test t1 throughout the entire range of $V_{l,t}$, whereas M^{DR} during tests t3, 6, and 12 are characterised by a steady decrease. Interestingly, at low $V_{l,t}$, M^{DR} values for t3 are slightly higher than for test t1; this may in part be due to some non-uniform deformation of the plate in the tunnel longitudinal direction.

Finally, it is important to evaluate the performance of simplified empirical TPI analyses described by Devriendt & Williamson (2011) based on the subsurface greenfield settlement profiles (i.e. DR_{gf} at z/L_p=2/3). As displayed by the dashed lines in Figures 5c, d, relating the modification factors to DR_{gf} at z/L_p=2/3 resulted in $M^{DR,sag}$ and $M^{DR,hog} < 1.0$. In particular, during test t12, $M^{DR,sag} < 0.5$ and $M^{DR,hog} = 0$ for DR_{gf} measured at z/L_p=2/3. Therefore, these centrifuge tests confirmed that this damage assessment should be conservative.

4 CONCLUSIONS

The paper described a series of centrifuge tests performed to study the response of piled buildings to tunnelling. The following conclusions can be drawn.

- Piles alter the input of tunnel-structure interaction (i.e. the greenfield soil movements) and can have a detrimental role in TPSI problems. Piled foundations lead to the narrowing of the building settlement curve in case of fully-flexible structures because of the pile interaction with subsurface soil movements. This increases the deflection ratio and the potential for damage to flexible buildings.
- The superstructure stiffness affects the building distortions resulting from tunnelling (both deflection ratios and horizontal strains). Piled buildings respond critically to tunnelling in term of flexural deformations, whereas horizontal strains in buildings that are continuous at the ground level are negligible even in the case of low axial stiffness.
- In general, assuming the building as a fully flexible structure (i.e. performing a TPI analysis) can lead to the overestimation of the superstructure *DR*. In particular, using subsurface greenfield settlement curves at z/L_p=2/3 (i.e. DR_{gf} at z/L_p=2/3) leads to a marked overestimation of *DR* in case of relatively stiff structures and could be conservative even for very flexible structures.
- The increase of $V_{l,t}$ should decrease the building distortions measured relative to the greenfield case with M^{DR} because of soil stiffness degradation.
- The overall building settlement is dependent on the building self-weight and the residual safety factor of the piles (i.e. the ratio between residual ultimate and serviceability load). Experiments indicated that the overall magnitude of the building settlement due to tunnelling may increase with the increase of building self-weight. This is probably due to the loads transferred by the superstructure from the piles above the tunnel to the external ones, thereby exceeding the residual bearing capacity of the external piles. Further work is planned where the effects of building self-weight and stiffness are better isolated.

REFERENCES

Basile, F. 2014. Effects of tunnelling on pile foundations. *Soils & Found.*, 54(3): 280-295.

Devriendt M. & Williamson, M. 2011. Validation of methods for assessing tunnelling-induced settlements on piles. *Ground Eng.*: 25–30.

Goh, K.H. & Mair, R.J. 2014. Response of framed buildings to excavation-induced movements. *Soil & Found.*, 54 (3): 250-268.

Fargnoli, V. Gragnano, C.G. Amorosi, A. and Boldini, D. 2015. 3D numerical modelling of soil-structure interaction during EPB tunnelling. *Géotechnique*, 65 (1): 23-37.

Farrell, R. Mair, R. Sciotti, A. & Pigorini, A. 2014. Building response to tunnelling. *Soils & Found.*, 54(3): 269-279.

Franza, A. & Marshall, A.M. 2015. Semi-analytical prediction of ground movements due to shallow tunnels in sand. In: *Proc. XVI ECSMGE Geotech. Eng. Infrastr. & Develop.*: 461-466.

Franzius, J.N. Potts, D.M. & Burland, J.B. 2006. The response of surface structures to tunnel construction. *Proc. Inst. Civ. Eng. Geotech. Eng.*, 159(1): 3-17.

Giardina, G. DeJong, M.J. & Mair, R.J. 2015. Interaction between surface structures and tunnelling in sand: Centrifuge and computational modelling. *Tunnelling and Underground Space Technology*, Vol. 50, 465-478.

Mair, R.J. & Williamson, M.G. 2014. The influence of tunnelling and deep excavation on piled foundations. In: *Proc. 8th Int. Symp. Geotech. Aspects Undergr. Constr. Soft Ground*: 21-30.

Marshall, A.M. Farrell, R.P. Klar, A. & Mair, R. 2012. Tunnels in sands: the effect of size, depth and volume loss on greenfield displacements. *Géotechnique*, Vol. 62 (5): 385-399.

Marshall, A.M. & Mair, R. 2011. Tunneling beneath driven or jacked end-bearing piles in sand. *Canadian Geotech. J.*, 48(12):1757-1771.

White, D.J. Take, W.A. & Bolton, M.D. 2003. Soil deformation measurement using particle image velocimetry (PIV) and photogrammetry. *Géotechnique*, Vol. 53 (7): 619-631.

Zhou, B. Marshall, A.M. & Yu, H.S. 2014. Effect of relative density on settlements above tunnels in sands. In: *Proc. 2014 GeoShanghai Int. Congress*: 96-105.